Master WAPE - Module MEC558 “Continental hydrology and water resources”

Personal Research Project

Estimation of Surface Latent Heat Flux With Bulk Method

Student: Diyin LU

Tutor: Agnès Ducharne

1. Introduction

Latent heat flux, which corresponds to evapotranspiration from land surface, is a subject of interest in atmospheric boundary layer (ABL) study. Basically, the evaporation from land and ocean surfaces happens in the surface layer and thus corresponds to a turbulent flux. Following turbulent theory we can apply Reynolds decomposition to split a quantity into the mean and fluctuating parts:

$$x = \bar{x} + x' \tag{1}$$

where $\bar{x}$ is the mean value of the quantity while x’ represents turbulent fluctuation ($\overline{x'} = 0$).

When applying this decomposition to turbulent transport of moisture in the atmospheric surface layer:

$$F_{vz} = \rho(\bar{q}\bar{w} + \overline{q'w'}) \qquad [\text{kg.m}^{-2}.\text{s}^{-1}] \tag{2}$$

The first term in the bracket represents vertical transport of water vapor by the mean motion and the second one by the turbulence. As mean vertical velocities are small in front of the horizontal ones, the first term equals to 0, left only:

$$\overline{F_{vz}} = \rho\overline{w'q'} \qquad [\text{kg.m}^{-2}.\text{s}^{-1}] \tag{3}$$

Under steady conditions above a uniform surface, on account of continuity, the inflow rate equals the outflow rate, and the vertical fluxes must be constant with height z. Ground surface is a source for water vapor, via the evaporation at surface:

$$\overline{F_{vz}} = \rho\overline{w'q'} = E = \rho\overline{w'q'_0} \qquad [\text{kg.m}^{-2}.\text{s}^{-1}] \tag{4}$$

where the subscript 0 denotes the value near the surface.

Over the last decade, eddy covariance has been applied as a main method in measuring surface

latent heat flux. It is based on the direct measurement of $\overline{w'q'}$ of the equation above, with Reynolds means over periods of 5 minutes to 1 h at most, and Reynolds fluctuations measured with a frequency of at least 5-10 Hz. However, in absence of such instrument, we need alternative means to estimate latent heat flux.

The bulk aerodynamic method is regarded as one of such alternatives for latent heat estimation. Within the general framework of turbulence similarity, the basis for bulk method is to replace the mean product of temporal fluctuations by the product of the spatial changes of the corresponding mean quantities:

$$\overline{w'q'} \simeq -C_x(\overline{u_2} - \overline{u_1})(\overline{q_4} - \overline{q_3}) \tag{5}$$

where the subscripts 1 to 4 refer to measurement heights above the surface, Cx is a dimensionless parameter depending on measurements levels 1 to 4 and other factors. $\overline{u}$ is used as the mean horizontal wind speed (in the sense of Reynolds). For Evaporation E, the equation writes as:

$$E = \rho_a \overline{w'q'} = -\rho_a C_e \overline{u} \triangle \overline{q} \qquad [\text{kg.m}^{-2}.\text{s}^{-1}] \tag{6}$$

The dimensionless transfer coefficients Ce is drag coefficient for water vapor, equals to:

$$C_e = \frac{k^2}{\ln(z_2 / z_0)\ln(z_1 / z_{0v})} \tag{7}$$

This equation works in neutral atmosphere conditions, under such conditions, the wind profile in the atmosphere over flat homogeneous terrain increases logarithmically with height which is closely related to the momentum flux (Gordon B Bonan, 2002). The subscripts 1 and 2 refer to the measurement height of wind speed and specific humidity respectively, z0 is called momentum roughness length corresponding to the height at which wind speed is 0, its value can be either experimentally defined or estimated as about 10% of the average height of the vegetation. z_{0v} is the height at which specific humidity get its surface value. Generally, for water vapor and sensible heat fluxes it can be assumed that $z_{0v} \approx 0.1$ zo. k is commonly referred to as von Karman's constant, and dimensional analysis shows that:

$$k = -\frac{E}{\rho z u_* (d\overline{q} / dz)} = \frac{u_*}{z(d\overline{u} / dz)} \tag{8}$$

where u* is friction velocity, used to express shear stress. By eliminating u*, we finally get:

$$E = \frac{-\rho k^2 \overline{u}_{(zu)}[\overline{q}_{(zj)} - \overline{q}_{(zi)}]}{\ln(z_u / z_0)\ln(z_j / z_i)} \qquad [\text{kg.m}^{-2}.\text{s}^{-1}] \tag{9}$$

Evaportranspiration E can be deduced from latent heat flux that $LE=2.501*10^6$ with $L=2.501*10^6$

J.kg-1, the latent heat of vaporization at standard pressure. Thus, the bulk method can be applied to compute latent heat flux, given horizontal wind velocity at level z_u, and specific humidity at two levels z_i and z_j. The only unknown variable in this equation is roughness length z_0, so the key point of this research is the retrieval of z_0 by inversing this equation, given latent heat flux from EC measurement. By analyzing and calibrating z_0, we could then simulate latent heat or evapotranpiration from wind speed u at z_u, specific humidity at z_i and z_j when EC method doesn't work.

2. Data and observation site

The research project makes use of 3 months measurement data collected at SIRTA site from 1st June to 31th August 2012 (92 days). SIRTA (Site Instrumental de Recherche par Télédétection Atmosphérique) is a French national atmospheric observatory dedicated to cloud and aerosol research. It is located in Palaiseau (49°N, 2°E), 20 km south of Paris (France) in a semi-urban environment (Haeffelin, M et al., 2005). Observation data mainly comes from the measurement of 2 flux towers situated in the same site but several tens of meters away from each other. For the whole 92 days, we have complete profile of air temperature and relative humidity at 5 heights (1m, 2m, 5m, 10m, 20m, 30m), wind speed at 10m and 30m (the latter only obtained at the end of the work), ground temperature and humidity at 4 different depths underground (-5cm, -10cm, -20cm, -50cm), atmospheric pressure, radiation (both incoming and outgoing, shortwave and longwave) at 10m. We also have 2 sets of eddy covariance data: one at 30m above the surface (called LMD), for which we only have latent and sensible heat from 9th August to 25th August (16 days); the other is at 2m (called IPGP) for which we can only use data from 15th to 25th August (10 days). As latent heat flux is indispensable in retrieving z0, the analysis is mainly focused on the 16-day period with available LE data.

2.1 General meteorological conditions during the observation period

2.1.1 Net radiation

The net radiation (Rn) at the Earth's surface consists of the incoming shortwave, outgoing shortwave, incoming longwave and outgoing longwave radiation:

$$Rn = SW\downarrow - SW\uparrow + LW\downarrow - LW\uparrow \qquad [W.m^2] \qquad (10)$$

With all the components on the right side known at 10m, the net radiation at 10m can be obtained, see figure 1.

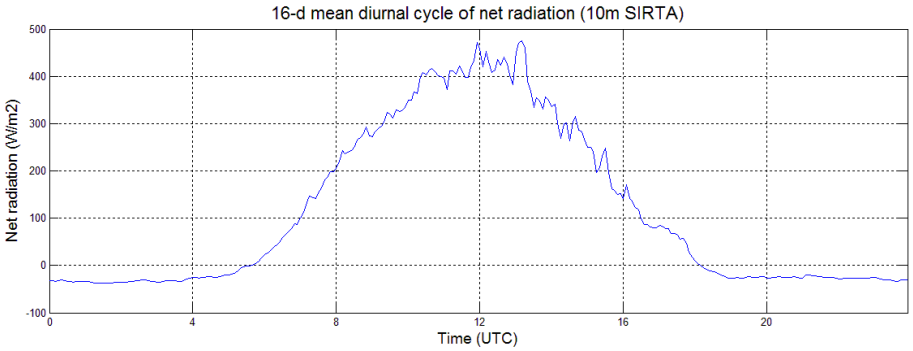

Figure1. Mean diurnal cycle of net radiation at 10m

For the 16 days of observation, net radiation is positive during day time and reaches maximum around 12 am. The slightly negative value in the night indicates a net loss of radiation from surface to the air. However, the day time gain and night time loss are not equal, for the whole day, the surface receives more energy than it lost to atmosphere through radiation.

2.1.2 Air temperature

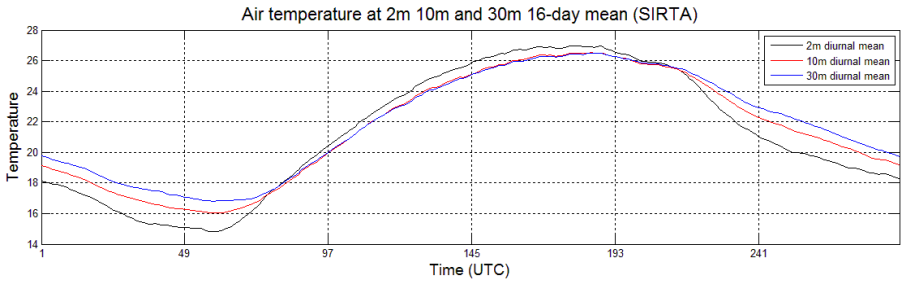

Figure3. 16-day mean diurnal cycle of air temperature at 2m 10m and 30m

The pattern of mean diurnal cycle of temperature is just opposite to air density: maxima when density is minimum and minimum when density is maxima. Comparing the temperature at 3 different heights (2m, 10m, 30m), it is observed that 10m and 30m temperature are very close but a little higher at 30m during the night. 2m temperature is highest during the day but smallest at night. This is consistent with our knowledge that at day time with ground absorbing solar radiation more efficiently, air is heated from the ground surface while at night, the ground cools down more than the air.

2.1.3 Air density

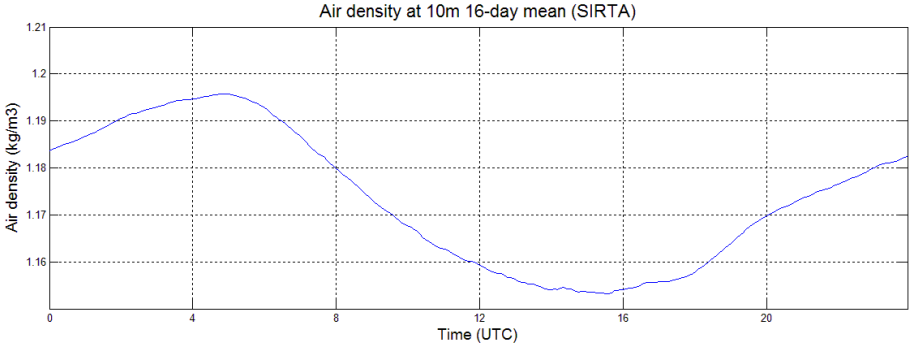

Figure2. Mean diurnal cycle of air density at 10m

Diurnal cycle of air density has a very steady and sinusoidal shaped regime, at 10m high, density is largest around 5-6 am and smallest around 3-4pm. The value decreases after sunrise and increases again after 4pm.

2.1.4 Wind speed

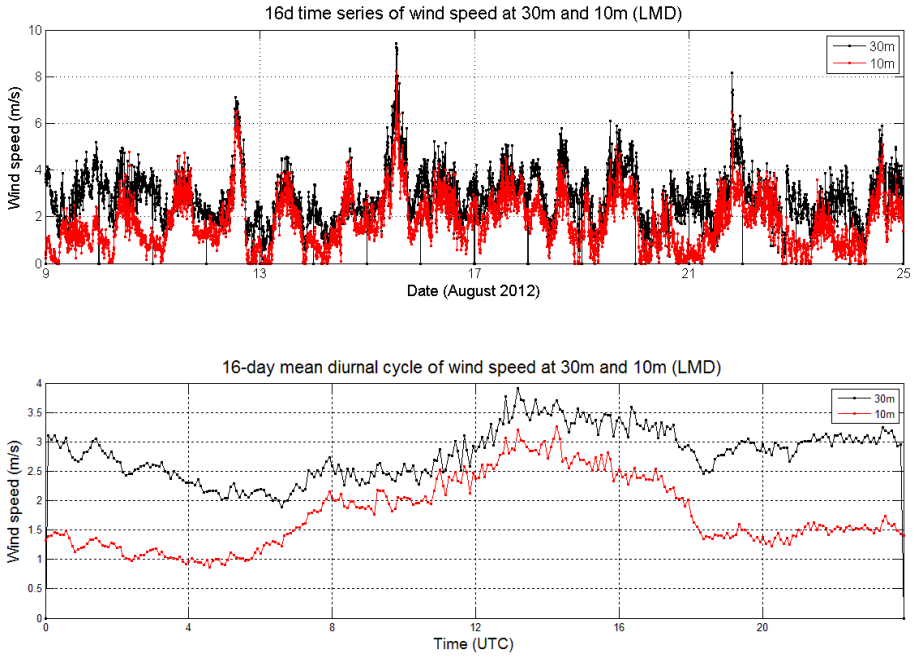

Figure4. 16-day time series and mean diurnal cycle of wind speed at 10m and 30m

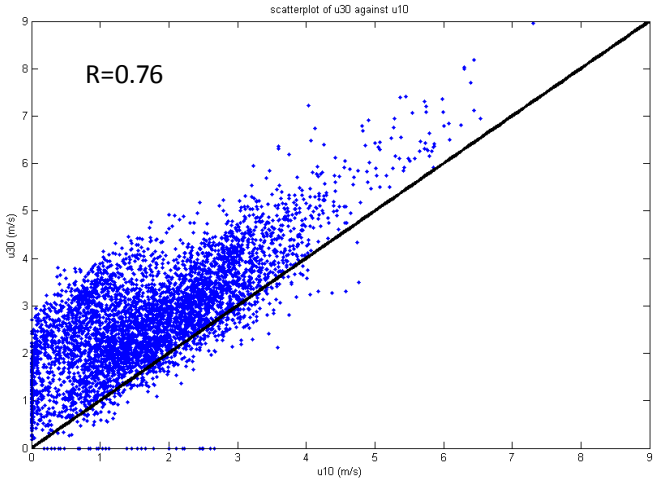

Figure5. Scatterplot with correlation coefficient of wind speed at 10m and 30m

Wind speed at 10m is between 1m/s to 3m/s, at 30m is between 2m/s to 4m/s, it is normal that u10<u30 since wind speed undergo logarithmic decrease with height in the dynamic boundary

layer under neutral conditions because of the friction. Their diurnal cycles have similar trend and variation, with values are both higher (with smaller discrepancy) around the noon and lower at night (with larger discrepancy).

2.1.5 Atmospheric humidity

Observations provide the relative humidity at several levels, we need to follow a series of computation to get the specific humidity used in bulk formula.

Saturated water vapor pressure is the function only of air temperature (in Kelvin unit):

$$e_s = 6.112 \exp\left(\frac{17.62T}{T + 243.12}\right) \quad \text{[hpa]} \tag{11}$$

Actual water vapor pressure is further obtained:

$$e = e_s * RH / 100 \quad \text{[hpa]} \tag{12}$$

Specific humidity depends on actual water vapor pressure and air pressure:

$$q = \frac{0.622e}{p} \quad \text{[kg/kg]} \tag{13}$$

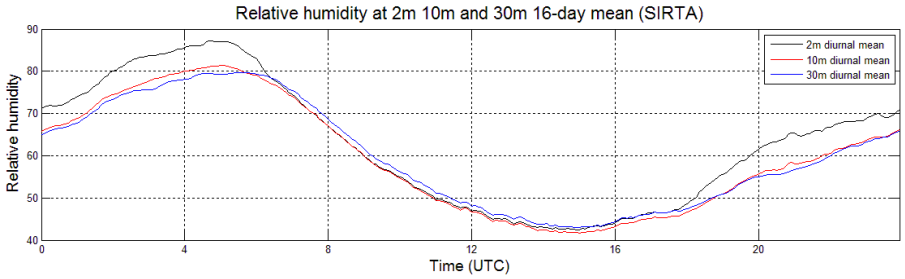

Figure6. Mean diurnal cycle of relative humidity at 2m 10m and 30m

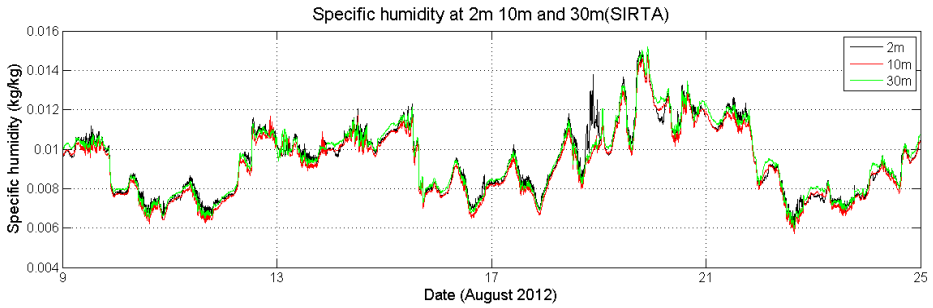

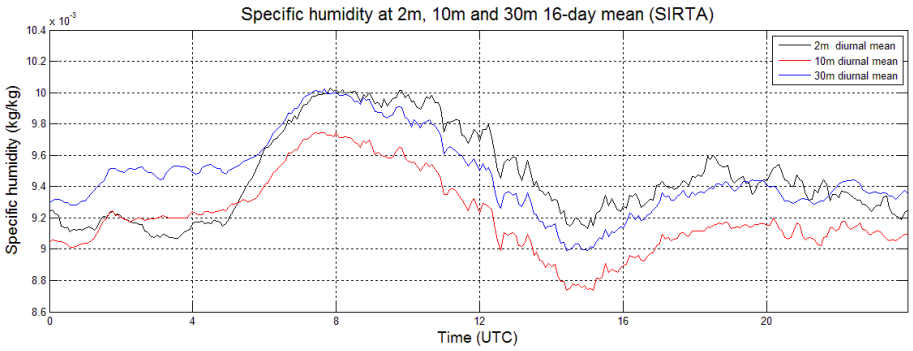

Figure7. Time series (upper) and diurnal cycle (lower) of specific humidity at 2m 10m and 30m

Observing the full time series of specific humidity of the 16 days, the values at three different levels are rather consistent except for 18th August when there is a large discrepancy of the value at surface with at higher levels, this may be due to sudden storm in the afternoon which is very common in summer. However there is no record of such storm from the precipitation data which may be caused by the measurement error of either relative humidity or precipitation or other unknown synoptic process.

Studying the diurnal cycle, it is found that specific humidity is highest in the morning (around 8 am) and lowest in the afternoon (around 3pm), maybe due to the high surface evaporation with temperature increase in the morning as well as sufficient water supply (condensed water at night) from ground surface which is somehow exhausted after long time evaporation in the afternoon, the largest specific humidity doesn't coincide with the maximum latent heat flux which peaks at noon (fig. 9) as the latter also dependent on turbulence. The temperature decreases before dusk and soon equilibrium is reached between evaporation and condensation.

There is also a reduction of specific humidity with increasing height except at night when the surface specific is the lowest, which reflects a night time inversion (related to negative values of LE in Fig 9). Yet, it is noticeable that specific humidity at 30m is always higher than at 10m, the difference between the 2 levels is almost constant all the day without any inversion. This phenomenon is far from our expectation since ground surface is considered as the source of water vapor, so that it is unusual to have a larger specific humidity at higher level than at lower level without knowing any constant source of water supply. The advection between the height 10m to 30m is probably an explanation for this since it implies that the vertical fluxes are in opposite direction between 2 and 10m, and between 10 and 30m, while the starting assumption is that the flux is vertically constant. It can also be that the different sensors are not correctly intercalibrated.

2.1.6 Temperature gradient

Inversion is closely connected with atmospheric stability. Generally, air is much more stable at night than in the day time because heat flux exchange is reduced at night, dampening the turbulence which is a major contributor in breaking the stability. Air stability depends on the vertical rate of temperature decrease, also known as the atmospheric lapse rate. In absence of water phase change, the dry air adiabatic lapse rate is defined as:

$$\Gamma_d = g / c_{pd} \simeq 9.8 K.km^{-1} \quad (14)$$

We can compute the vertical temperature gradient as:

$$\Gamma = -(T_j - T_i) / (z_j - z_i) \quad \text{[k/km]} \quad (15)$$

Since air is unsaturated (Fig. 6), we can compare this gradient with the dry adiabatic lapse rate of dry air, to decide the stability condition:

If $\Gamma > \Gamma_d$, air is unstable

$\Gamma = \Gamma_d$, is neutral condition

$\Gamma < \Gamma_d$, stable condition

In this study, temperature gradient between 2m and 30m is computed, figure 8 is the comparison of mean diurnal cycle of this temperature gradient with adiabatic lapse rate of dry air.

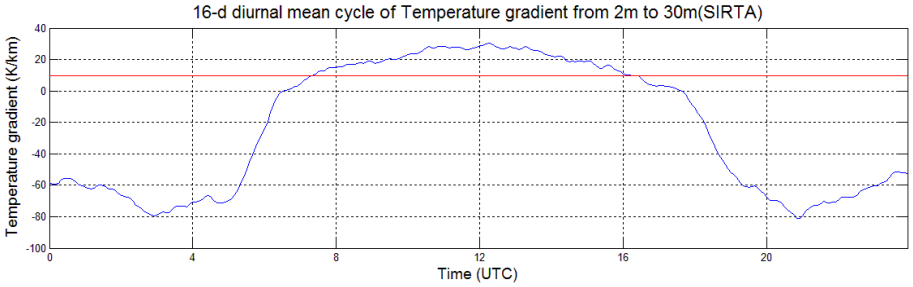

Figure8. diurnal cycle of temperature gradient from 2m to 30m

Temperature gradient is strongly negative at night, which indicates very stable condition that gives rise to significant nighttime inversion, and it is larger than the adiabatic lapse rate positive at daytime, which indicates unstable conditions, favoring vertical turbulent motion.

2.1.7 Sensible and latent heat flux

We have available heat flux observations at 30m from 9th to 25th August, but for at 2m only from 15th to 25th August, we compare the 2 sets of data for the same 10 days:

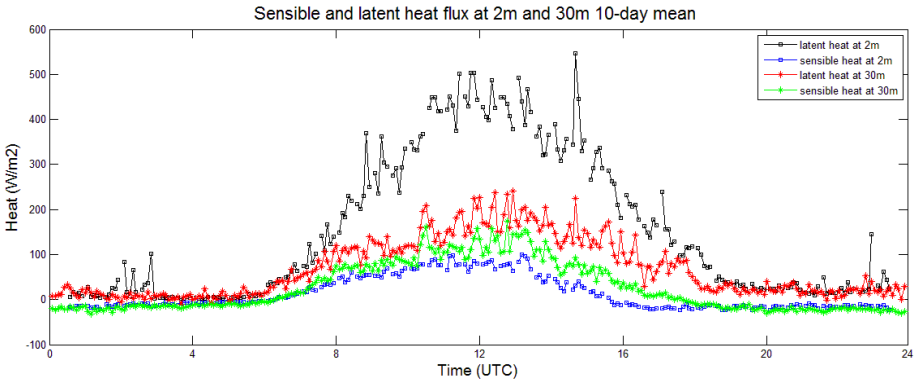

Figure9. diurnal cycle of sensible/latent heat flux at 2m and 30m

Both latent heat and sensible heat at the 2 heights exhibit clear diurnal cycle: close to 0 and rather stable at night, increase from sunrise and peak in noon then decrease toward night. The values of sensible heat flux and latent heat flux are close to each other at 30m, with latent heat always a little higher. Near the surface, latent heat is much higher than sensible heat during daytime with the largest discrepancy at noon, however they are almost the same at night. Measurement of heat flux have very large variation, at 30m, the latent heat flux varies from -377 W/m^2 to 627 W/m^2 with mean value of 88W/m^2. At 2m, the range is 0 to 1656 W/m^2 and the mean value is 159 W/m^2. The results of 2m measurement are very problematic because it is impossible that latent heat is larger than solar constant (less than 1400 W/m^2). Another problem is that the latent and sensible heat fluxes are not constant within the lowest 30m, which is not consistent with the assumptions of the bulk method. Since the measurement of heat flux at 2m IPGC only has 10d available data with a lot missing point (mainly at noon and midnight), and associated with such uncertainties, this research project mainly makes use of the heat flux at 30m but occasionally use 2m heat flux data for comparison.

3. Roughness length estimation

3.1 Method 1: direct computation

Using the bulk method, we can directly retrieve z_0 following Eq. 9, which can be re-arranged:

$$z_0 = z_u / \exp[\frac{-\rho k^2 \bar{u}_{(zu)}[\bar{q}_{(zj)} - \bar{q}_{(zi)}]}{E * \ln(z_j / z_i)}] = z_u / \exp[\frac{-2.501*10^6 \rho k^2 \bar{u}_{(zu)}[\bar{q}_{(zj)} - \bar{q}_{(zi)}]}{LE * \ln(z_j / z_i)}] \quad (17)$$

To perform this method, we need to choose a combination of q(zj), q(zi) and LE to compute. As described before, we have specific humidity at 3 levels (2m, 10m and 30m) with latent heat flux measured by EC instrument at 2 levels (2m and 30m). However, from figure 7, we already know that specific humidity at 30m is larger than 10m and for a long period even larger than at 2m, which is not consistent and doesn't favor the application of bulk method. Thus we use the specific humidity combination of 2m (q2) and 10m (q10) as well as the latent heat flux value at 30m as set 1, the combination of 2m (q2) and 30m (q30) with also latent heat flux at 30m

(discussed in the previous part) as set 2 in this study.

Furthermore, if the 10m wind speed is 0, we always get z0=10, which is meaningless because z0 is the height at which positive above-ground wind speed is reduced to 0, and given the condition of SIRTA, this value should be far smaller than 10. Neglecting all the z0=10, with set 1, we get 4457 available results but in which there are many very large or infinite values: 38% belong to the range [0, 1), 43% belong to [1, 10), 7% to [10, 100), 12% are even larger than 100. Seeing the probability distribution, incredibly large results exist which are purely numerical faults.

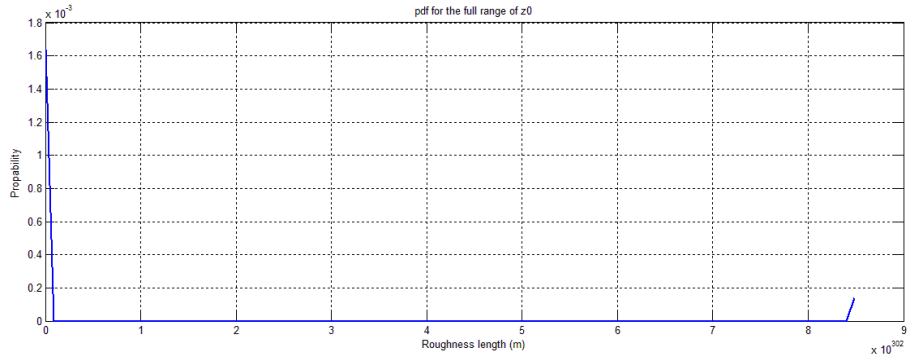

Figure10. probability distribution of estimated z0 from set 1

If we look into the formula, we can find if the ratio: $(\overline{q_{zj}} - \overline{q_{zi}}) / LE$ is positive and very large, the denominator exp($(\overline{q_{zj}} - \overline{q_{zi}}) / LE$) is close to zero leading to infinite value of z0. To avoid this numerical problem, we neglected all the data with $(\overline{q_{zj}} - \overline{q_{zi}}) / LE$ >0. After this step (Fig. 11), all the results left in set 1 (3669 in total, 80% of the original data) are smaller than 10 ([0, 9.9475]), the average value is 2.23m. For set 2, 2611 (only 57% of the original data) are left after the remove and the average value is 4.42m.

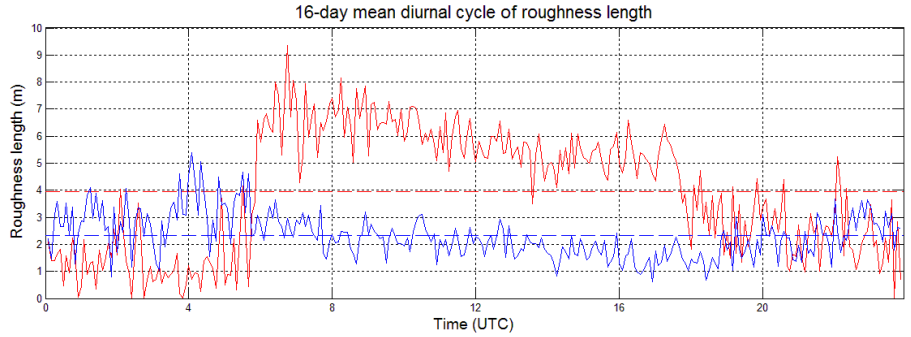

Figure11. Comparison of mean diurnal cycle (solid line) and avarage value (dashed line) of roughness length computed with set 1 (blue line) and with set 2 (red line)

With 2m and 10m specific humidity, the estimated roughness length has small variation, which is what we expect; the value is slightly higher than the average (2.23m) at night and lower in the day time. However, situation is very different with the results from q2 and q30 combination, the

estimated roughness length shows very large variation with higher mean value (3.94). Roughness length is much smaller at night than during day time, particularly, we notice there is sudden change during transition time (around 6 am and 6 pm). This difference is supposed to be related to the specific humidity difference given other variables exactly the same (equation-17). Given the short grassland coverage at SIRTA, this result is rather high, the surrounding forest and buildings may have effects on the roughness length.

3.2 Method 2: bulk regression

As direct computation using bulk method results in large uncertainty with a lot numerical errors due to the equation itself, an alternative way to use this method while avoiding such error as well as diminishing the influence of random large fluctuations of measurement or other uncertainties is to perform a regression analysis.

Let y=LE, x= $-\bar{u}\rho(\bar{q}_{zj}-\bar{q}_{zi})$ zi<zj, qzi>qzj

We can then assume that y=ax with $a=\dfrac{2.501\times10^{6}k^{2}}{\ln(z_j/z_i)\ln(z/z_0)}$

By regressing latent heat flux against the parameterized variable x, we can obtain a, value of the slope. Then the roughness length can be calculated following the underlying relation:

$$z_0 = z/\exp\left(\frac{k^2}{a\ln(z_j/z_i)}\right) \quad \text{[m]} \qquad (18)$$

Again following the analysis in direct computation, regression is applied with set 1 and set 2 respectively (we also remove the unacceptable data as in the direct computation):

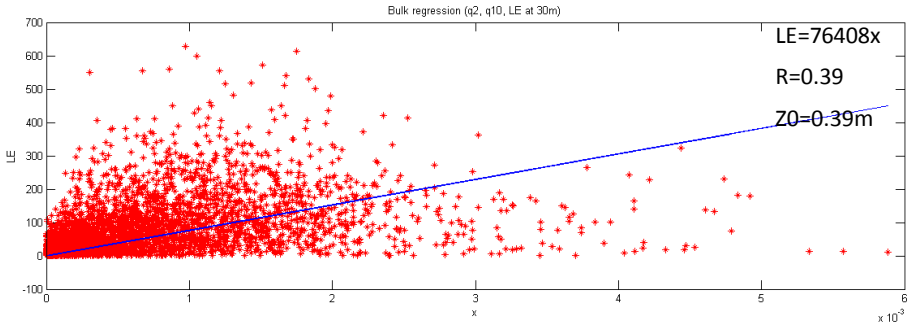

Figure12. Regression with q2 q10 and LE at 30m

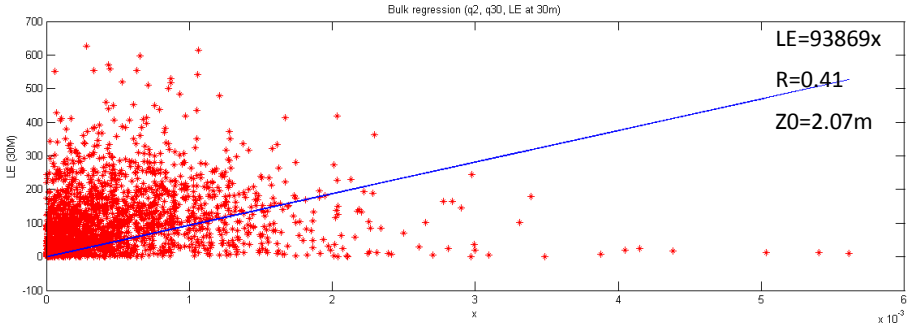

Figure13. Regression with q2 q30 and LE at 30m

The correlation coefficients are not very good. The estimated roughness length are smaller than from direct computation especially for set 1. The difference of specific humidity between 2m and 10m is larger than between 2m and 30m, with smaller difference in set 2, we get larger roughness length (2.07) and slightly higher correlation (0.41). The latent heat we have is at 30m high, this may explain the higher correlation in this case.

3.3 Method 3: Logarithm wind profile regression

With wind speed at 2 different heights, we can perform linear regression of height against wind speed to retrieve roughness length. In neutral conditions:

$$\bar{u}(z) = \frac{u_*}{k}\ln(\frac{z}{z_0}) \qquad [m.s^{-1}] \qquad (19)$$

This equation is based on the theory that wind velocity decreases linearly with the decrease of ln(z), the value of z when wind speed vanishes to 0 is the roughness length, therefore, we can use extrapolation to compute z0. Time series and diurnal cycle of the results can be seen from figure 14.

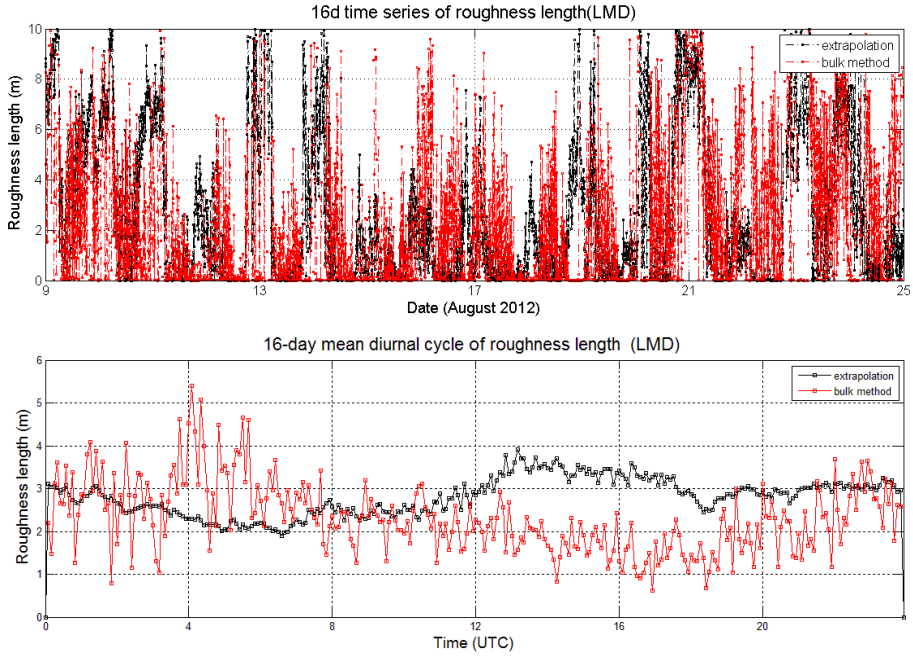

Figure14. Comparison of time series and diurna cycle of estimated z0. Red color represents results from mehtod 1 bulk computation (set 1), black represents results from logarithm wind profile regression

The average value of wind profile regression is 2.66m with standard deviation of 2.95, this result is higher than from bulk regression and most close to direct computation with set 1 (q2 to q30). However, if we compare these their results (wind profile method and bulk method with set 1,

figure14), no explicit correlation can be seen between them except the values are mostly confined between 1 to 4, in contrast, their trends seem to be opposite to each other particularly around transition time of sunrise and sunset. Results from bulk method have larger variation and amplitude than from wind profile regression. Bulk method is based on the latent heat difference (thus evapotranspiration) which is less stable with larger amplitude compared with wind speed difference used in regression, furthermore, wind profile regression is a rather simplified method without many uncertainties as in bulk method which is very sensitive to small change of variables.

4 The impact of atmospheric stability

It should be kept in mind that the prerequisite of all the methods discussed here is a neutral condition. According to the previous discussion (section 2.1.6), temperature inversion at night is very common during the observation period while in daytime there is strong convection inducing unstable situation. Another criterion for atmospheric stability is given by the bulk Richardson number. When measuring wind shear and temperature gradients, meteorologists approximate the gradients by measurements at discrete heights:

$$Ri = \frac{g}{\overline{T}} \frac{(T_j - T_i)(z_j - z_i)}{(u_j - u_i)^2} \tag{20}$$

This Bulk Richardson Number characterizes the stability of the air as:

Ri>0, stable

Ri=0, neutral

Ri<0, unstable

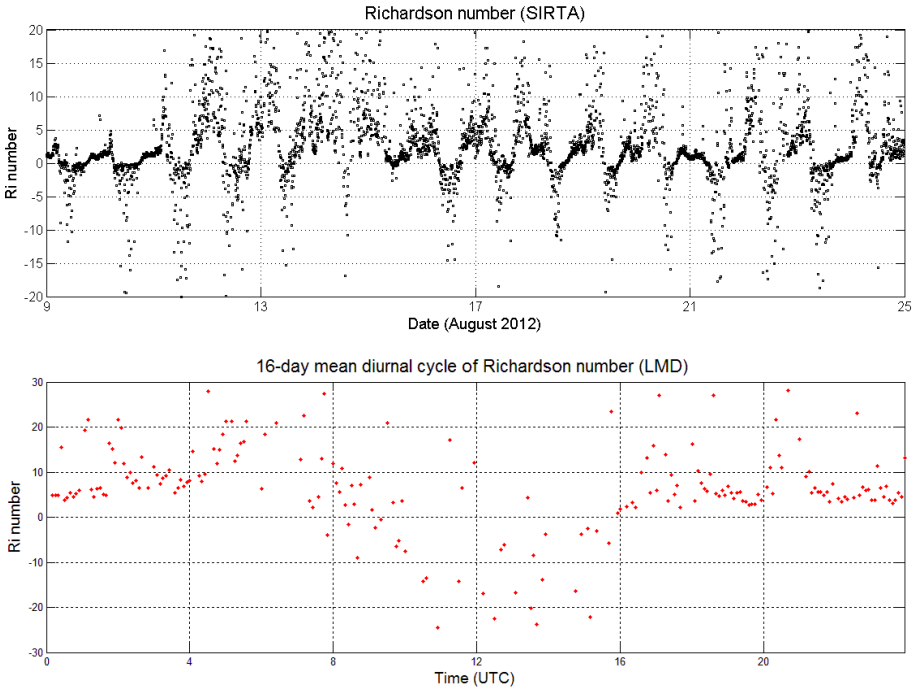

Figure15. Time series (upper) and diurnal cycle (lower) of Ri number

Richardson number exhibits very large variations, strongly negative or very large values are common, judging from the mean diurnal cycle, Ri is only close to zero around 8am and 4pm during a day, otherwise the condition can be very stable or very unstable. This result confirms the findings in temperature gradient analysis.

4.1 reexamination of z0 from bulk method (method 1)

In this project, we reexamined the roughness length from bulk method according to the 3 conditions: Ri smaller than -5 is considered as very unstable, larger than 5 is very stable and within [-5, 5] is close to neutral condition.

Table 1. Comparison of estimated z0 from bulk method by regrouping data with respect to air stability

Ri	**number**	**SET 1**		**number**	**SET 2**	
		Z0	Std		Z0	std
(-∞,-5)	397(11%)	2.03	2.10	361(14%)	2.51	2.88
[-5,5]	2322(64%)	2.46	2.67	1619(62%)	4.67	3.36
(5,+ ∞)	895(25%)	1.75	2.43	631(24%)	3.14	3.41
total	3614	2.23	2.56	2611	4.42	3.39

Roughness length is largest in neutral condition and smaller in either stable or unstable condition for both sets, however, the value is larger in unstable condition than in stable in set 1 computation (with q2 - q10, LE at 30m) but opposite in set 2.

4.2 Reexamination of z0 from bulk regression method (method 2)

We applied again bulk regression while dividing points in 3 groups with different Ri values, see figure 16-21 the regression and all the results are summarized in table 2.

Table 2. Comparison of estimated z0 from bulk regression by regrouping data with respect to air stability

Ri	**number**	**SET 1**	**number**	**SET 2**

		Z0	R		Z0	R
(-∞,-5)	397(11%)	0.69	0.04	361(14%)	3.44	0.02
[-5,5]	2322(64%)	0.33	0.36	1619(62%)	1.92	0.36
(5,+ ∞)	895(25%)	0.29	0.43	631(24%)	0.69	0.47
total	3614	0.39	0.39	2611	2.07	0.41

With increasing Richardson number, using bulk regression method we find the roughness length decreases while the correlation increases when the atmosphere condition becomes more and more stable. Contrasting with direct computation method, the 2 sets of results are quite consistent with each other.

Compared with neutral condition, z0 is larger in unstable condition and smaller in stable condition. Bulk method assumes neutral condition, if it is not the case, z0 is larger when unstable (day time) but smaller when stable (night time). This is logical since in stable condition, less turbulence induces lower drag forcing, thus lower roughness length (see equation 7), while unstable condition is associated with higher z0.

4.3 Reexamination of z0 from logarithm wind profile method

Wind profile regression is also reexamined based on this criteria, see table 3:

Table 3. Comparison of estimated z0 from wind profile regression by regrouping data with respect to air stability

Ri	**Number**	**mean $Z_{0\,(m)}$**	**std**
(-∞,-5)	408 (9%)	0.12	0.61
[-5,5]	2868 (62%)	3.17	3.02
(5,+ ∞)	1332 (29%)	2.03	2.66
total	4608	2.66	2.95

We get unexpected results when discussing roughness length with respect to the stability of the atmosphere. 9% of roughness length resulted from extrapolation are under unstable condition (Ri < -5), the mean value is 0.12; 22% are under neutral condition -5=<Ri=<5, the mean value is 3.17;

60% are under stable condition Ri>5, with mean value equals to 2.03. Given the assumption that this method works in neutral condition, it is most likely the roughness length be around 3m which is close to the result from direct computation of bulk method. With wind profile regression method, roughness length is underestimated when unstable condition and overestimated in stable condition, which is opposite to the case of bulk regression method (as can be seen in figure 14). The value of roughness length and standard derivation are both smallest in unstable condition (Ri<-5), however, largest when close to neutral condition (-5=<Ri=<5).

Following all the methods, 3 groups of results are obtained. It is noticed that roughness length around 2m is an acceptable result for all the methods performed here, it is associated with lower standard deviation in direct computing or higher correlation coefficient in regression. Therefore, z0=2.07 from regression (method 2 or 3?, set 2, q2-q30) is taken to simulate latent heat flux at 30m. The simulation result is compared with the observation (figure 22).

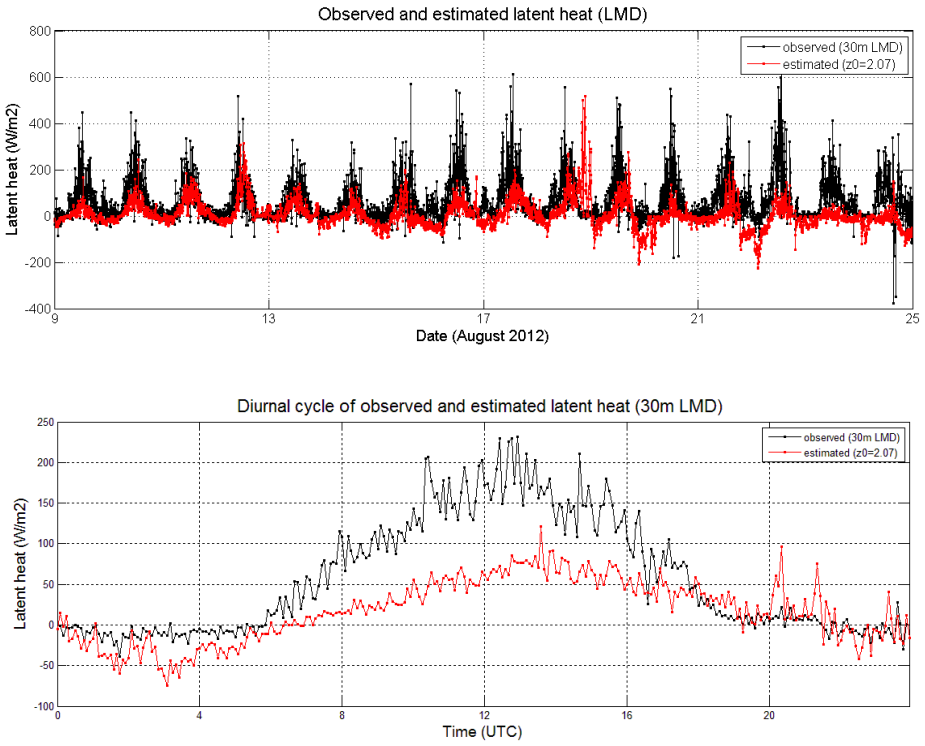

Figure22. Comparison of time series (upper) and diurnal cycle (lower) of estimated and observed LE

The estimated latent heat flux is systematically undersestimated during day time to as much as 100% at noon. Even though it is more consistent with the measurement at low value (night time), while their discrepancy is larger at high value (daytime). As bulk method is based on the assumption of neutral condition but as analysed above, the condition is only neutral around 7am and 5pm, there is strong stability at night but strong instability at daytime, this may suggest that bulk method works better in neutral or stable condition but can significantly underestimate the latent heat in unstable condition except on 18 August which is due to the sudden increase of relative humidity which is analysed before.

5 Energy balance closure

Energy balance closure is an important test of eddy covariance data, it is directly relevant to the evaluation of latent and sensible heat fluxes (Anderson et al., 1984; Mahrt, 1998). The formulation of energy balance closure requires that the sum of latent and sensible heat flux be equivalent to all other energy sinks and sources:

$$LE+H=Rn-G-S-Q \quad (21)$$

where Rn is the net radiation, G the heat flux into the soil, S the rate of change of heat storage in a very thin surface layer, and Q the sum of all additional energy sources and sinks usually present in the canopy, for instance, photosynthesis is a form of biochemical energy storage (Kell Wukson et al., 2002). In this reach, the term S and Q are neglected with the attention only focused on radiation, heat flux and the heat into the soil, we have:

$$G=Rn-LE-H \quad (22)$$

With the available data, the G plus energy budget residual at SIRTA is examined and plotted here:

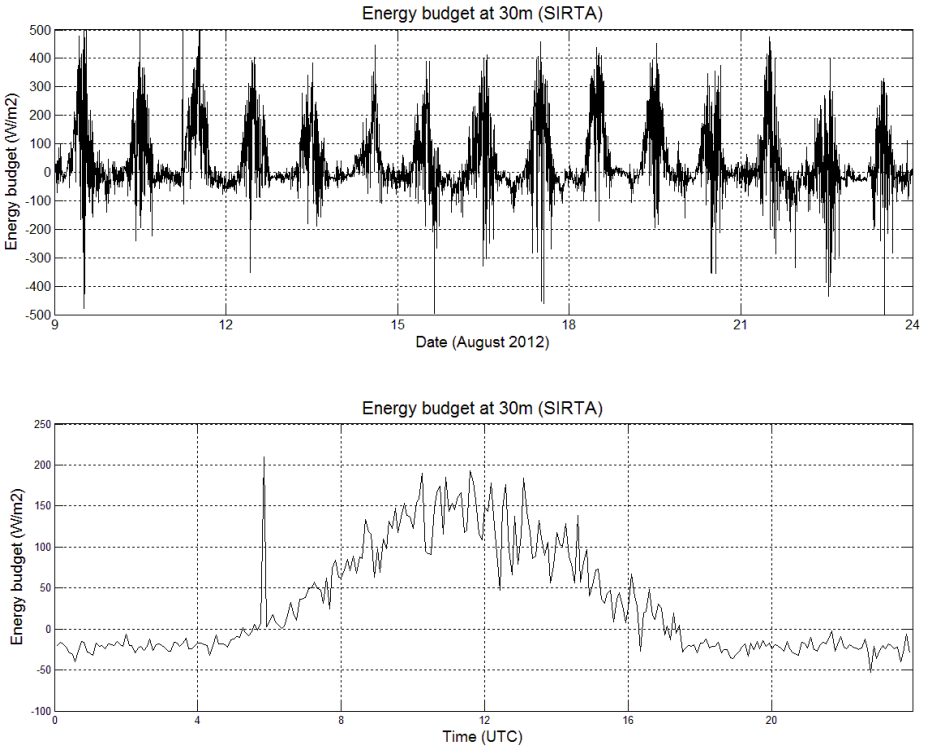

Figure23. Time series (upper) and diurnal cycle (lower) of energy budget at 30m

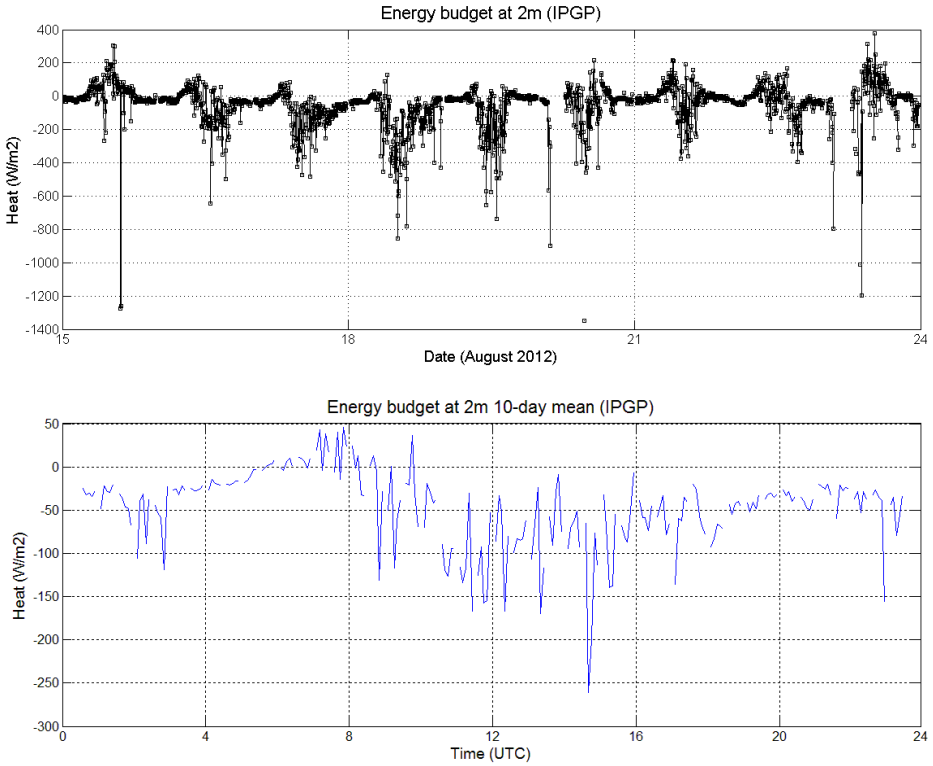

Figure24. Time series (upper) and diurnal cycle (lower) of energy budget at 2m

For the same 10 days, daily mean value of $Rn-LE-H$ is 22 W/m^2 at 30m (LMD), -46W/m^2 at 2m (IPCG). The 2m measurement has much more noise and shows more uncertainty than at 30m. In our assumption, the daily mean of G should be small in front of the other variables however the results we get from the observations, either 22 W/m2 or -46W/m2 are not close to 0 which we have expected. Their opposite signs may be related to the fact that latent and sensible heat fluxes are not constant with height (Fig. 9). Furthermore, one must keep in mind that the net radiation is measured at 10m height, while heat fluxes are measured at 2m and 30m respectively. The outgoing heat flux is larger near the surface than at higher level since basically ground surface is the source of heat fluxes, and the actual net radiation at 2m and 30m can be different from at 10m, also taking account of unknown sinks or sources due to horizontal advection or convection between different heights, these together can somehow explain the inconsistent of Rn-LE-H value at 2m and 30m.

Heat into the soil is an important term in energy balance closure formulation, as the balance between sensible and latent heat flux and net radiation is not verified, we need to analysis soil temperature profile to see if soil is a sink/source of surface heat flux that is needed to account for.

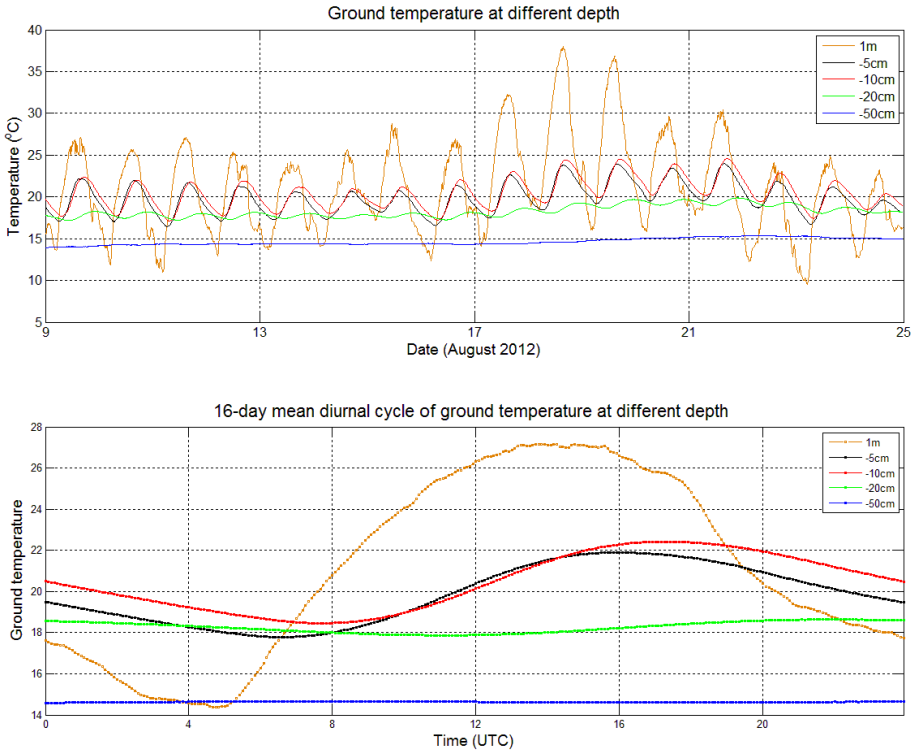

Figure25. Time series (upper) and diurnal cycle (lower) of ground temperature at different depth

It can be seen from the figure of ground temperature at different depths that the temperature slightly increases from the surface to -10cm during the night time and then a great decrease downward. Near the surface (-5cm and -10cm), soil temperature has a clear diurnal change which is similar to air temperature profile (Fig. 3) but with a lag of 2-3 hours. At day time, surface temperature is much higher than the ground but air temperature decreases much more than the ground temperature at night because of the heat capacity difference. These findings confirm that the heat flux is transferred to the ground from the surface and the net G is positive during the day but negative at night, however it is still not enough to quantify the net value of G and to explain the contradicting results of heat flux measurement at 2m and 30m.

6 Conclusions and field works at SIRTA

The objective of this research project is to assess the tractability of the bulk aerodynamic method to estimate latent heat flux in a case study with a wealth of data, including the measurement of LE from an eddy correlation system. The estimation of roughness length ends up being the key point of study, together with the analysis of the measurements' consistency. Inverse computation is performed to retrieve z0 and 3 methods used here are bulk method of direct computation, bulk method of parameterization and regression and logarithm wind profile regression. The results from different methods vary from 0.39 to 4.42 (average value). Bulk regression results in smaller roughness length value than direct computation. With specific humidity at 30m, the results are higher than use specific humidity at 10m when other variables are the same. The analysis of general meteorological profile in SIRTA shows atmosphere is very unstable at daytime and very stable during the night with frequent inversion. Based on the Richardson number, the impact of

air stability on roughness length estimation is studied. Roughness length is recomputed with respect to different atmospheric condition (unstable, neutral or stable) and the results are compared. Using bulk regression, we have large value of z0 in unstable condition and smaller z0 in stable condition but opposite with logarithm wind profile method.

With the estimated z0 from bulk regression which is acceptable based on several criteria, we perform the simulations of latent heat flux at 30m and compare the simulations with observations, the comparison shows that this estimation works better in neutral or stable condition but significantly underestimate the flux. The energy balance closure is studied in the end, and suggests that there is no energy conservation using the observed data, even though heat flux into the soil can somehow explain this disequilibrium between net radiation and heat fluxes.

From the quality control analysis, we find that the observation data of SIRTA is problematic, especially for the heat flux measurement. Apart from the many missing timesteps without measurement, results from the two flux towers are not consistent or even contradicting. It is hard to tell whether the uncertainty and large fluctuation of heat flux are due to measurement error or meteorological variability.

Besides the data analysis, I also participated in practical works at SIRTA site as part of the training project. The two EC systems that provide data in this research are not consistent with each other and we need to intercalibrate them. We reset the one at 30m close and horizontally parallel to the one IPGP at 2m. By comparing the measurement of the 2 we may better understand the measurement uncertainty as well as the data quality of this project.

Reference：

[1]Anderson D E, Verma S B, Rosenberg N J. Eddy correlation measurements of CO2, latent heat, and sensible heat fluxes over a crop surface[J]. Boundary-Layer Meteorology, 1984, 29(3): 263-272.

[2]Bonan G B. Ecological climatology: concepts and applications[M]. Cambridge University Press, 2002. 207-201.

[3]Haeffelin, M., L. Barthès, O. Bock, C. Boitel, S. Bony, D. Bouniol, H. Chepfer, M. Chiriaco, J. Cuesta, J. Delanoë, P. Drobinski, J-L. Dufresne, C. Flamant, M. Grall, A. Hodzic, F. Hourdin, F. Lapouge, Y. Lemaître, A. Mathieu, Y. Morille, C. Naud, V. Noël, B. O'Hirok, J. Pelon, C. Pietras, A. Protat, B. Romand, G. Scialom, R. Vautard, 2005: SIRTA, a ground-based atmospheric observatory for cloud and aerosol research." Annales Geophysicae, 23, pp 253-275.

[4]Mahrt L. Flux sampling errors for aircraft and towers[J]. Journal of Atmospheric & Oceanic Technology, 1998, 15(2).

[5]Wilson K, Goldstein A, Falge E, et al. Energy balance closure at FLUXNET sites[J]. Agricultural and Forest Meteorology, 2002, 113(1): 223-243.